Modeling and Numerical Simulation of Material Science, 2023, 13, 29-49
https://www.scirp.org/journal/mnsms
ISSN Online: 2164-5353
ISSN Print: 2164-5345

Modal and Thermal Analysis of a Modified Connecting Rod of an Internal Combustion Engine Using Finite Element Method

Nkrumah Jacob Kwaku[1], Baba Ziblim[2], Sulemana Yahaya[3], Sherry Kwabla Amedorme[4]

[1]Automotive Engineering Research Institute, Jiangsu University, Zhenjiang, China
[2]Department of Automotive Engineering, Tamale Technical University, Tamale, Ghana
[3]Department of Mechanical Engineering, Tamale Technical University, Tamale, Ghana
[4]Department of Mechanical and Automotive Engineering, Akenten Appiah-Menka University of Skills Training and Entrepreneurial Development, Kumasi, Ghana
Email: jnkrumah@tatu.edu.gh

How to cite this paper: Kwaku, N.J., Ziblim, B., Yahaya, S. and Amedorme, S.K. (2023) Modal and Thermal Analysis of a Modified Connecting Rod of an Internal Combustion Engine Using Finite Element Method. *Modeling and Numerical Simulation of Material Science*, **13**, 29-49.
https://doi.org/10.4236/mnsms.2023.133003

Received: June 21, 2023
Accepted: July 22, 2023
Published: July 25, 2023

Abstract

The connecting rod is one of the most important moving components in an internal combustion engine. The present work determined the possibility of using aluminium alloy 7075 material to design and manufacture a connecting rod for weight optimisation without losing the strength of the connecting rod. It considered modal and thermal analyses to investigate the suitability of the material for connecting rod design. The parameters that were considered under the modal analysis were: total deformation, and natural frequency, while the thermal analysis looked at the temperature distribution, total heat flux and directional heat flux of the four connecting rods made with titanium alloy, grey cast iron, structural steel and aluminium 7075 alloy respectively. The connecting rod was modelled using Autodesk inventor2017 software using the calculated parameters. The steady-state thermal analysis was used to determine the induced heat flux and directional heat flux. The study found that Aluminium 7075 alloy deformed more than the remaining three other materials but has superior qualities in terms of vibrational natural frequency, total heat flux and lightweight compared to structural steel, grey cast iron and titanium alloy.

Keywords

Connecting Rod, Steady-State Thermal Analysis, Deformation, Heat Flux, Thermal and Modal, Finite Element Method

1. Introduction

The internal combustion engine consists of different components one of which is the connecting rod that connects the piston to the crankshaft. The core function of the connecting rod is to transmit force from the gudgeon pin to the crankpin by converting the reciprocating motion of the piston into rotary motion of the crankshaft. The connecting rod has two ends: the big end which connects it to the crankpin and the small end which is connected to the piston by means of the gudgeon pin [1]. The connecting rod has a long shank which can be designed to take the form of rectangular, tubular, circular, I-section, and H-section. The circular section is generally used on slow-speed engines while the I-section is used on high-speed engines [2]. The I-section is both lightweight and strong, but the type of material used limits its capacity to handle load. Whereas H-section can handle much more stress without bending, so, they are used in high power engines [3] [4]. The connecting rod should be able to sustain the gas load or be strong enough to withstand buckling load at both x-axis and y-axis when subjected to alternating direct compressive and tensile loads [5]. The compressive loads impose on the connecting rod are much higher than the tensile loads, therefore the cross-section of the connecting rod is designed as a strut and Rankine's formula is used to determine the dimensions of the connecting rod [6] [7] [8]. Manufacturers of automobiles are striving hard to reduce the weight and cost of the vehicle to optimise speed and reduce excessive energy loss and therefore the current study intends to design a connecting rod for weight reduction. To support and be part of the advocates of weight reduction of the automobile, Dupare Y. B. *et al.* [9] indicated that their design of connecting rod using a different material has led to a reduction of 3.05% of weight of the original connecting rod. Several researchers such as [8] [10] also obtained maximum weight reductions in using different materials to manufacture connecting rods, without affecting the main structural parameters. In this regard, different materials for connecting rod designs are usually analysed and compared using static structural analysis to understand the variations of equivalent von-mises stress, strain, total deformation and factor of safety in the materials [11] [12]. The possibility of re-engineering the connecting rod to reflect the modern trends of engine design and development cannot be over-emphasized. In the view of Balli S. R., *et al.* [13] connecting rods are most usually made of steel for automobile engines, but can be made of aluminium alloy for lightness, affordability, and to absorb high impact. As such, they compared aluminium alloy 6065, magnesium alloy, titanium alloys (Ti-3Al-2.5V), and beryllium alloy (25) in order to find the best material for connecting rod manufacture. Their study revealed that apart from titanium alloy, aluminium 6065 has equally superior properties for connecting rod design. Furthermore, in the domain of aluminium alloy itself, three different aluminium alloy materials such as AA2014, AA6061, and AA7075 were evaluated by Fukuda s., and Eto H [14]. Comparing the results of these three materials showed that Al alloy 2014 possesses less weight and better stiffness. Buddi *et al.* [15] also shared their opinion on their design and pointed out that bringing Si3N4 into Aluminium composite improved the material properties in view of the good similarities and the interfacial grip between the Si3N4 and the aluminium framework. Connecting rod has been a subject of research and many researchers have written extensively on connecting rod design and manufacture using various combinations of materials, but little has been said about the comparative study of materials such as Aluminium Alloy 7075, which is also a possible connecting rod material, hence the motivation behind this study to investigate the possibility of using aluminium 7075 for connecting rod design. Heat conductivity is an important parameter that must be considered when selecting a material for connecting rod design and manufacture since the connecting rod is exposed to high temperature in the combustion chamber of an internal combustion engine. Aluminium alloys are known for their lightweight nature but their capacities to withstand high temperature vary from one aluminium alloy to another. According to Ajit, and Ravindra [16] indicated that, employing transient thermal analysis on connecting rods using finite element analysis in their study revealed that Al 6060 materials have more value of heat flux compared with different other materials and therefore suggested that Al 6060 material be used for connecting rods in the future. In a similar study conducted by Sunny *et al.* [17] where three different materials (S-460, ALG-HS 1300 and Al Si 398) were used the results showed that AlSi 398 material has more value of heat flux compared to the other materials. Three different materials such as structural steel, aluminium alloy, and titanium were also investigated to determine their suitability for connecting rods under steady-state thermal conditions. The results from the comparative studies using parameters such as temperature, total heat flux and directional heat flux distribution in the connecting rod showed that the Al alloy suffered less thermal deformation in the connecting rod [18] [19].

Significance and Novelty of the Study

It is important to bring out other materials that can be used to design and manufacture automotive components to reduce weight and cost. The automotive industry in Ghana over the years has grown sluggishly. This is because there was low skilled labour and lack of interest by successive governments to develop the automotive sector in Ghana. Almost everything concerning the automotive industry in Ghana was imported. The government of Ghana of recent past has initiated the drive to industrialise the automotive sector in the country through government policies and programmes. This country has so far seen a tremendous growth in the automotive industry of late. There is now an influx of automotive assembling companies in Ghana. Companies such as Kantanka motors, Toyota and VW motors are now assembling vehicles in the country. For this industrialisation drive to be successful in the country there is the need for highly skilled automotive engineers to take the centre stage. Government through the ministry of trade and industry has brought forth the one district one factory policy to further enhance the industrialisation drive. The current President of Ghana is preaching Ghana beyond aid agenda. This agenda seeks to encourage local manufacturers to use the raw materials in the country to produce products and encourage Ghanaians and companies within Ghana to patronise locally produced goods to spare the country's forex market from changing Cedis to Dollars for importation of goods. This research seeks to contribute towards governments' effort to developing the automotive industry in Ghana. To this end, the study explores the possibility of using local materials such as aluminium to design and manufacture a connecting rod for an internal combustion engine for the local automotive industry in Ghana. Ghana is one of the countries in the world that can boast of large bauxite deposits and in recognition of that, the country has way back established Volta Aluminium Company to process the country's bauxite to alumina and plans are far advance to setup integrated aluminium company in Ghana. This among others motivated the authors to go all out to establish the suitability of aluminium 7075 alloy for connecting road design and manufacture in Ghana.

2. Method and Materials

2.1. Material Properties

The implementing material (Aluminium 7075 alloy) is composed of 90.0% Al, 5.6% Zn, 2.5% Mg, 0.23% Fe, and 1.6% Cu, though these percentages nominally fluctuate depending upon manufacturing factors. Table 1 shows the properties of the selected material (Aluminium Al7075).

Table 1. Properties of the material (Al 7075).

Parameters	Value	SI Unit
Density	2.81	g/cm^3
Ultimate Tensile Strength	572	MPa
Tensile Yield Strength	480	MPa
Compressive yield Strength	607.9	MPa
Poisson's Ratio	0.33	
Young's Modulus	71.7	GPa
Shear Modulus	26.9	GPa
Shear strength	331	MPa
Thermal Conductivity	150	W/m·K
Fatigue Strength	159	MPa

The commonly known materials for connecting rod manufacturing are steel and its alloys, cast iron, titanium, and its alloys and other aluminium alloys. For this work, analysis of the connecting rod has been based on comparing connecting rod made of gray cast iron, titanium alloy and structural steel to a connecting rod made of aluminium alloy 7075. The parameters that were considered for this study are, deformation, natural frequency and heat flux. Table 2 shows the material properties of the three control materials for connecting rod design and manufacture to form basics for comparison.

Table 2. Properties of grey cast iron, titanium alloy and structure steel.

Materials	Tensile Yield strength (MPa)	Compressive Yield Strength	Tensile strength (MPa)	Density (Kg/m^3)	Poisson's ratio	Young's Modulus (MPa)	Thermal conductivity W/m·K
Grey Cast Iron	130	943 MPa	200	7196	0.3	170	53
Titanium Alloy	1207	848 MPa	1276	4840	0.31	116	21.6
Structural Steel	540	720 MPa	845	7900	0.3	210	60.5

2.2. Connecting Rod Design Calculations

Table 3 shows the specifications of the engine whose connecting rod was designed, modelled and manufactured.

Table 3. Engine specification and pressure calculations.

Vehicle Model:	Nissan NP 300 Pickup Double Cab 2.5 litres
Displacement:	2488 cc (cm^3)
Fuel type	Diesel
Maximum power	98 Kw at 3600 r.p.m
Maximum Torque	304 Nm at 2000 r.p.m
Compression ratio	16.5:1
Number of Cylinders	4
Cylinder bore and Stroke	100 mm × 114 mm
Gearbox:	5 Speed, manual

2.2.1. Forces Acting on the Connecting Rod

The connecting rod is designed by taking the force of the connecting rod (F_C) equal to the maximum force on the piston (F_P) due to gas pressure.

$$F_c = F_P = \frac{\pi D^2}{4} \times P = \frac{\pi (100)^2}{4} \times 6.32 = 49637.2 \text{ N} \quad (1.1)$$

The connecting rod is designed for buckling about the x-axis. The factor of safety is taken as 5.5, therefore the buckling load,

$$W_B = F_C \times F.S = 49637.2 \times 5.5 = 273005 \text{ N} \quad (1.2)$$

The radius of gyration of the section about the x-axis is,

$$K_{xx} = \sqrt{\frac{I_{xx}}{A}} = \sqrt{\frac{419t^4}{12} \times \frac{1}{11t^2}} = 1.78t \quad (1.3)$$

Length of crank, $r = \frac{\text{Stroke of Piston}}{2} = \frac{114}{2} = 57 \text{ mm}$

The length of the connecting rod is 2 × stroke(l) = 228 mm.

According to Rankine's formula, the buckling load about the x-axis is:

$$W_B = \frac{\sigma_c \times A}{I + a\left(\frac{l}{K_{xx}}\right)^2} \tag{1.4}$$

The compressive yield strength of the Aluminium alloy (Al7075) = 607.9 MPa

The young's modulus of the material (Al7075) = 71.7 GPa

The *a* component in (1.4) is calculated as:

$$a = \frac{\sigma_c}{\pi^2 \times E} = \frac{607.9 \times 10^6}{\pi^2 \times 71.7 \times 10^9} = \frac{607.9 \times 10^6}{7.0765 \times 10^{11}} = 8.59 \times 10^{-4} = 0.000859 \tag{1.5}$$

To obtain the thickness (*t*) of the connecting rod, using (1.4) is given as:

$$\begin{aligned} 273005 &= \frac{607.9 \times 11t^4}{1 + 0.000859\left(\frac{228}{1.78t}\right)^2} \\ &= \frac{273005}{607.9} = \frac{11t^2}{1 + 0.000859\left(\frac{51984}{3.1684t^2}\right)} = \frac{11t^2}{1 + \frac{44.654}{3.1684t^2}} \end{aligned} \tag{1.6}$$

(1.6) was simplified to:

$$t^4 - 40.82t^2 - 575.33 = 0 \tag{1.7}$$

Using the quadratic formula to solve the quadratic equation given in (1.7) gives:

$$t = \sqrt{51.905} = 7.2 \text{ mm} = 7 \text{ mm} \tag{1.8}$$

2.2.2. Dimensions of the I-Section of the Connecting Rod

The thickness of the flange and web of the section $t = 7$ mm;

Width of the section, $B = 4t = 28$ mm;

Depth of the section $H = 5t = 35$ mm.

These dimensions are at the middle of the connecting rod. The width (*B*) is kept constant throughout the length of the rod, but the depth (*H*) varies.

The depth near the big end or crank end is kept as $1.1H$ to $1.25H$.

$$H_1 = 1.2H = 42 \text{ mm}$$

The depth near the small end or piston end is kept from $0.75H$ to $0.9H$.

$$H_2 = 0.85H = 29.75 \text{ mm} \approx 30 \text{ mm}$$

Therefore,

Dimensions of the section near the big end = 42 mm × 28 mm and,

Dimensions of the section near the small end = 30 mm × 28 mm.

Since the connecting rod is manufactured by casting, therefore, the sharp corners are rounded off.

To determine whether the section chosen is satisfactory, then, $\frac{I_{xx}}{I_{yy}} = 3.2$

$$I_{xx} = \frac{419t^4}{12} = 83834.92 \text{ mm}^4$$

$$I_{yy} = \frac{131t^4}{12} = 26210.92 \text{ mm}^4$$

$$\frac{I_{xx}}{I_{yy}} = 3.198 = 3.2 \quad (1.9)$$

(1.9) is an indication that the section chosen is satisfactory.

2.2.3. Dimensions of the Crankpin or the Big End Bearing

Taking,

d_c = diameter of the crankpin or big end bearing;

l_c = length of the crankpin or big end bearing = $1.3d_c$;

P_{bc} = bearing pressure = 10.8 to 12.6 N/mm^2.

The load on the crankpin or big end bearing

$$= \text{Projected area} \times \text{Bearing pressure} \quad (1.10)$$

$$= d_c \times l_c \times P_{bc} = d_c \times 1.3d_c \times 12 = 15.6(d_c)^2$$

The crankpin or the big end bearing is designed for maximum gas force (F_P), therefore, equating (1.1) and (1.10) gives;

$$15.6(d_c)^2 = F_P = 49637.2$$

$$(d_c)^2 = \frac{49637.2}{15.6} = 3182$$

Therefore,

$$d_c = 56 \text{ mm} \quad (1.11)$$

The length of the crankpin is given as.

$$l_c = 1.3d_c = 72.8 \text{ mm} \approx 73 \text{ mm} \quad (1.12)$$

The big end has removable precision bearing shells or brass or bronze or steel with a thin lining (1 mm or less).

2.2.4. Dimensioning of the Piston Pin or Small End Bearing

Taking

d_p = diameter of the piston pin or small end bearing;

l_p = length of the piston pin or small end bearing = $2d_p$;

P_{bp} = bearing pressure = 15 N/mm^2.

The load on piston pin or small end bearing

$$= \text{projected area} \times \text{Bearing pressure} \quad (1.13)$$

$$= d_p \times l_p \times P_{bp} = d_p \times 2d_p \times 15 = 30(d_p)^2$$

The piston pin or the small end bearing is designed for the maximum gas force (F_p), therefore, equating (1.13) to the maximum gas force (1.1) gives,

$$30(d_p)^2 = 49637.2$$

$$\left(d_p\right)^2 = \frac{49637.2}{30} = 1654.57 \text{ mm}$$

$$d_p = \sqrt{1654.57} = 40.7 \approx 41 \text{ mm} \quad (1.14)$$

$$l_p = 2d_p = 2 \times 41 = 82 \text{ mm} \quad (1.15)$$

The small end bearing is usually a phosphor bronze bush of about 3 mm thickness.

The modified connecting rod is designed using Autodesk inventor 2017 software with the following specifications from the designed calculation (**Table 4**).

Table 4. Specifications of the connecting rod.

Serial No.	Connecting Rod Parameters (mm)
1	Thickness of the connecting rod (t) = 7
2	Width of the section ($B = 4t$) = 28
3	Height of the section ($H = 5t$) = 35
4	Height at the Big End (H_1) = 1.2H = 42
5	Height at the small end(H_2) = 0.85H = 30
6	Inner diameter of the Small End = 43
7	Outer diameter of the Small End = 55
8	Inner diameter of the Big End = 58
9	Outer diameter of the Big End = 104
10	Diameter of the bolt = 17
11	Thickness of the big end cap = 17
12	Length of connecting rod = 228
13	Crank pin diameter = 56
14	Length of crank pin = 73
15	Piston pin diameter = 41
16	Length of piston pin = 82

2.3. The Connection Rod Boundary Conditions

The thermal and modal analysis of the connecting rods made with the four different materials was done in Ansys software version 2020 R2. The big and the small ends of the connecting rods were the locations where the constant temperature was applied in the case of the thermal analysis as shown in **Figure 1**. With the modal analysis of the connecting rod as shown in **Figure 2**, the big end of the connecting rod was constraint at no-load condition. The parameters that were considered during the thermal and modal analysis were: total deformation, natural frequency and total heat flux.

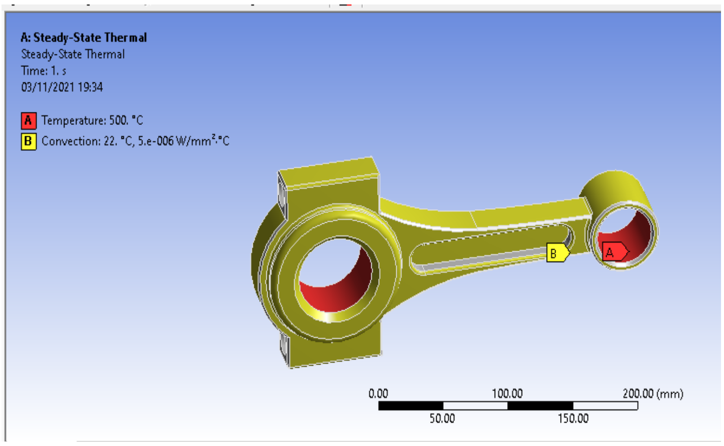

Figure 1. Boundary condition for thermal analysis.

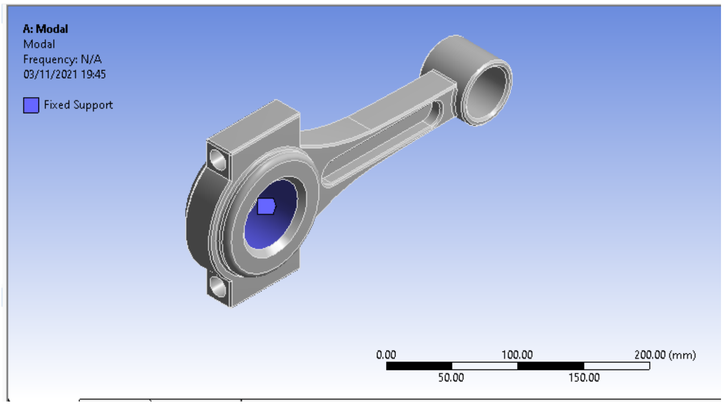

Figure 2. Boundary condition for modal.

2.4. Meshing of Connecting Rod

Meshing is a very important step in finite element analysis such as modal and thermal analysis processes. Meshing is an integral part of the engineering simulation process where complex geometries are divided into simple elements that can be used as discrete local approximations of the larger domain. Meshing influences the accuracy, convergence and speed of the simulation. If meshing is accurate, then the results are also anticipated to be closer to reality. The tetrahedral mesh details of the modelled connecting rods composed of 22,570 nodes and element size of 12,764. These sizes were arrived at after carrying out a grid independence test on the connecting rod. The meshing of the modelled connecting rod is as shown in Figure 3.

3. Results and Discussions

This section presents the simulated results on the thermal and the modal analysis for all the four (4) connecting rod materials, namely: titanium alloy, structural steel, grey cast iron and aluminium 7075 T6 alloy used in this work. It also discusses and compared the results to determine the best material for the connecting rod.

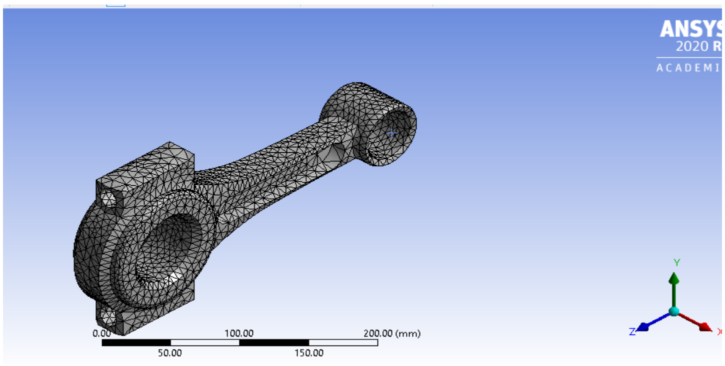

Figure 3. Connecting rod meshed in ansys.

3.1. Modal Analysis of the Connecting Rod

Modal analysis was run to determine the vibrational frequencies and the extent of deformation of the connecting rods of the four different materials. The modal analysis of the connecting rod means the free vibration analysis of the connecting rod in which the natural frequencies of vibrations are calculated at no-load conditions. The vibrational mode shapes, deformation and natural frequencies of the connecting rod when the modal analyses were conducted are presented in this section.

1) Titanium Alloy material

The data in Table 5 was extracted from Figure 4 and it shows the deformations and the natural frequencies when the modal analysis was performed on the connecting rod of titanium alloy material. It was observed from Table 5 that, the modal number with the highest deformation of 134.74 mm occurred in mode 9 corresponding to a natural frequency of 6114.5 Hz. It was also observed that mode 5 has the least deformation of 66.588 mm corresponding to a natural frequency of 2590.10 Hz. From Table 5, it was clear that the highest vibrational frequency of 7196.40 Hz corresponding to mode 10 has a lower deformation of 81.151 mm compared to some of the modes with lower frequencies. It is evident that as the mode number increases the natural frequencies also increase. It was again observed that the deformation of the connecting rod of titanium alloy material is not proportional to the magnitudes of the natural frequencies.

2) Structural Steel Material

Table 6 shows the deformations and the natural frequencies when the modal analysis was performed on the connecting rod of structural steel material. It was observed from Figure 5 as shown in Table 6 that the mode number with the highest deformation of 102.77 mm occurred in mode 9 corresponding to a natural frequency of 6847.7 Hz. It was also observed that mode 5 has the least deformation of 51.019 mm corresponding to a natural frequency of 2851.4 Hz. It can be deduced that the highest vibrational frequency of 7920.1 Hz corresponding to mode 10 has a low deformation of 60.697 mm compared to some of the modes with lower frequencies. It was again observed that the deformation of the connecting rod of structural steel is not proportional to the magnitudes of the natural frequency.

Table 5. Deformations and natural frequencies of connecting rod made with titanium.

Mode number	Titanium Alloy Material	
	Deformation (mm)	Natural frequency (Hz)
1	80.501	369.08
2	83.956	702.93
3	105.210	912.65
4	85.951	2125.90
5	66.588	2590.10
6	102.88	4023.00
7	107.91	4834.30
8	77.87	5670.90
9	134.74	6114.50
10	81.151	7196.40

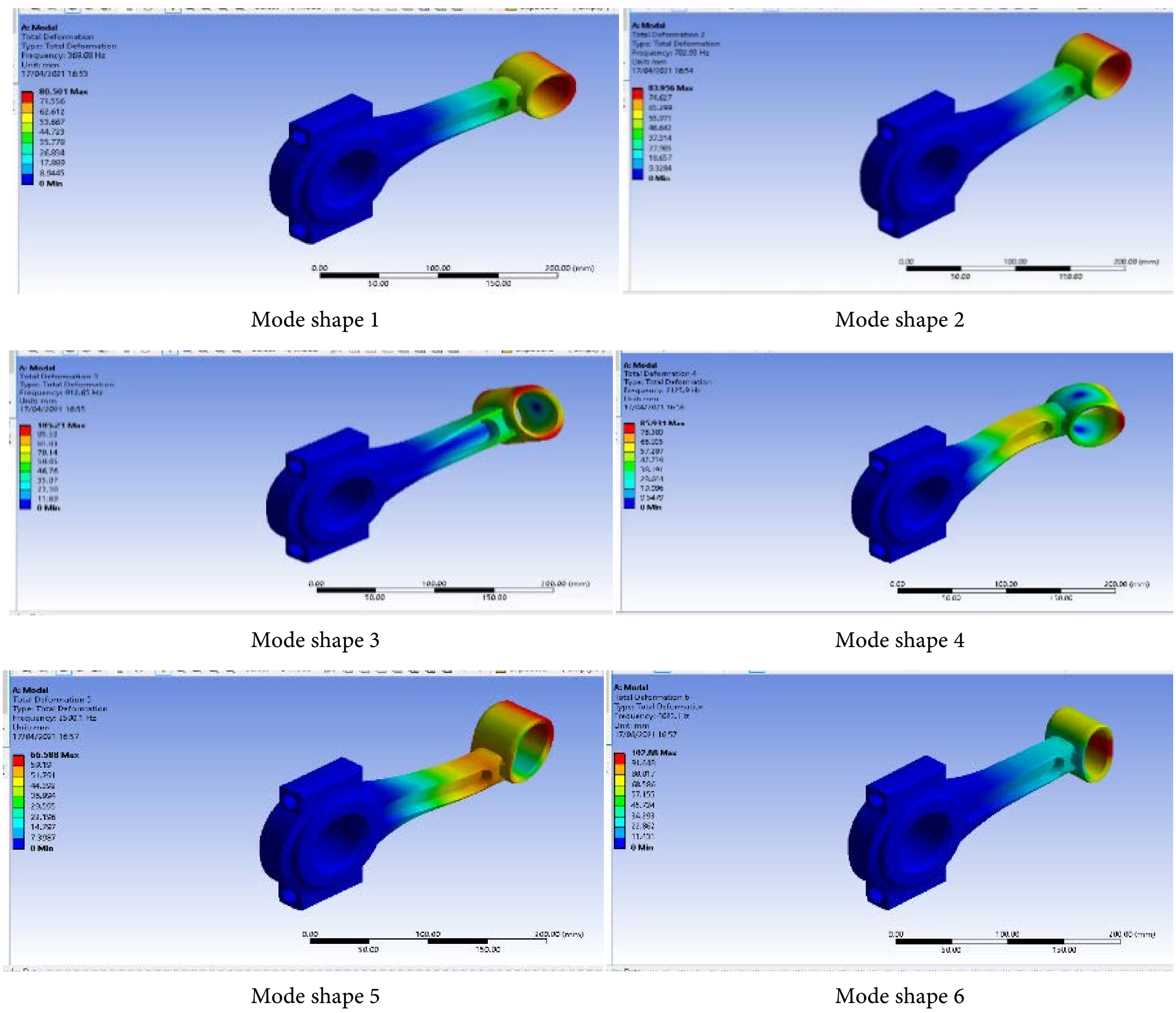

Mode shape 1 Mode shape 2

Mode shape 3 Mode shape 4

Mode shape 5 Mode shape 6

Figure 4. Mode shapes from 1 to 6 for Titanium.

Table 6. Deformations and natural frequencies of Con. rod of structural steel.

Mode number	Structural Steel Material	
	Deformation (mm)	Natural frequency (Hz)
1	61.754	408.3
2	64.552	777.4
3	80.687	1025.7
4	65.873	2353.9
5	51.019	2851.4
6	78.887	4415.6
7	82.123	5358.1
8	59.029	6303.7
9	102.77	6847.7
10	60.697	7920.1

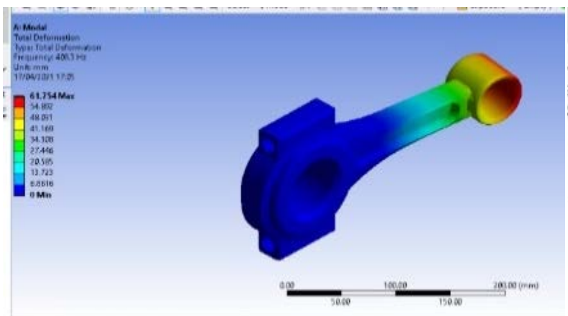

Mode shape 1

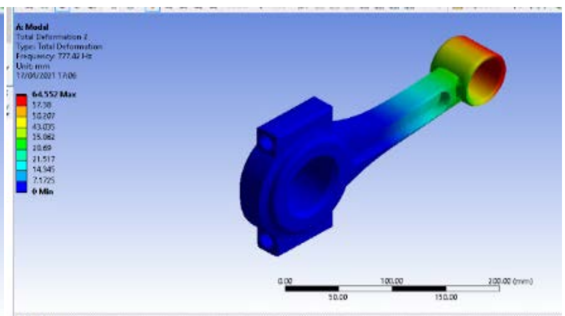

Mode shape 2

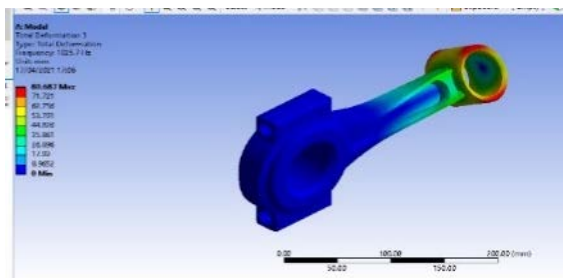

Mode shape 3

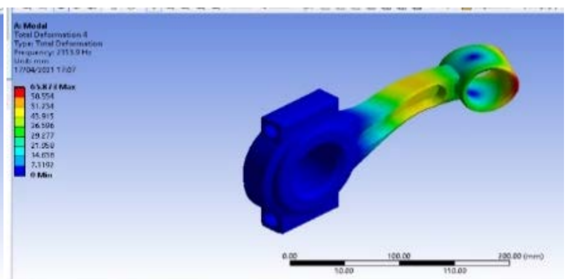

Mode shape 4

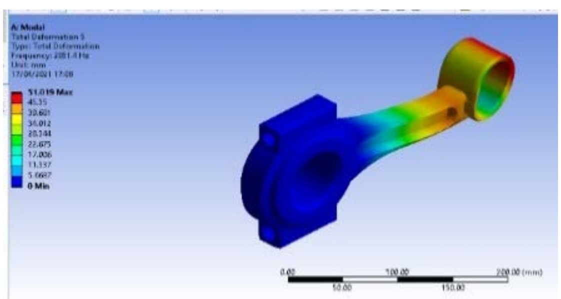

Mode shape 5

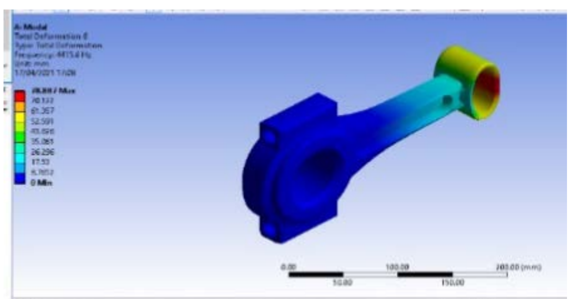

Mode shape 6

Figure 5. Mode shapes from 1 to 6 for structural steel.

3) Gray cast iron material

In the same vein, the data in Table 7 was extracted from Figure 6 which shows the deformations and the natural frequencies when the modal analysis was performed on connecting rod of gray cast iron material. It was observed that the mode number with the highest deformation of 107.11 mm occurred in mode 9 corresponding to a natural frequency of 5324.00 Hz. It was also shown that mode 5 has the least deformation of 53.249 mm corresponding to a natural frequency of 2204.70 Hz. It was clear that the highest vibrational frequency of 6123.00 Hz corresponding to mode 10 has a low deformation compared to some of the modes with low frequencies. It was again observed that the deformation of the connecting rod of gray cast iron material is not proportional to the magnitudes of the natural frequencies.

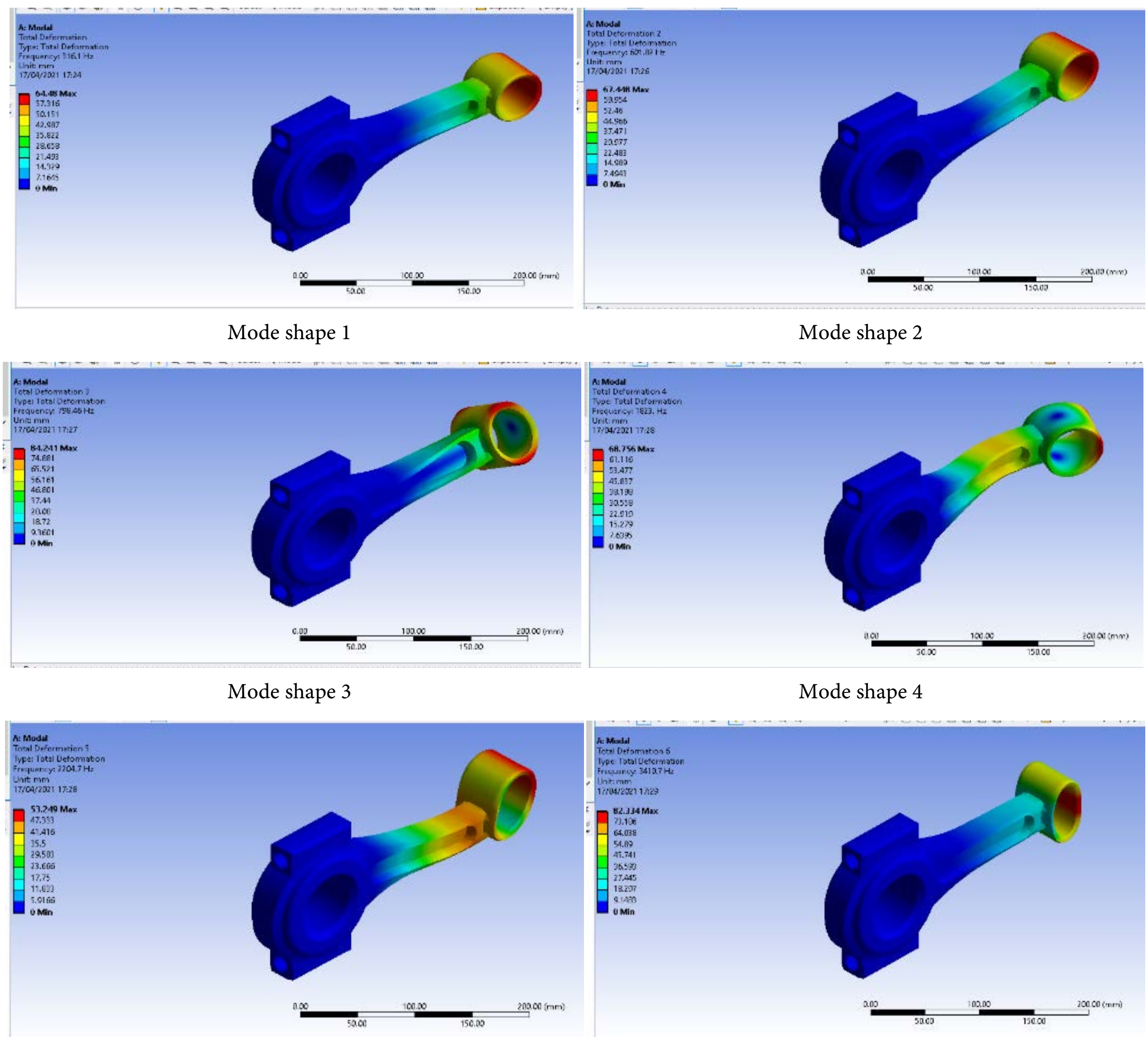

Mode shape 1 | Mode shape 2 | Mode shape 3 | Mode shape 4 | Mode shape 5 | Mode shape 6

Figure 6. Mode shapes from 1 to 6 for gray cast iron.

Table 7. Deformations and natural frequencies of Con. rod of gray cast iron.

Mode number	Gray Cast Iron Material	
	Deformation (mm)	Natural frequency (Hz)
1	64.480	316.10
2	67.448	601.82
3	84.241	798.46
4	68.756	1823.00
5	53.249	2204.70
6	82.334	3410.70
7	85.515	4151.80
8	61.395	4888.80
9	107.11	5324.00
10	62.90	6123.00

4) Aluminium 7075 alloy

Similarly, the data in Table 8 was extracted from Figure 7 which also shows the deformations and the natural frequencies when the modal analysis was performed on connecting rod of Aluminium 7075 T6 alloy material. The mode number with the highest deformation of 172.44 mm occurred in mode 9 corresponding to a natural frequency of 6820.50 Hz. It was also observed that mode number 5 has the least deformation of 85.419 mm corresponding to a natural frequency of 2864.20 Hz. It was observed that the highest vibrational frequency of 7957.00 Hz corresponding to mode 10 has a lower deformation of 102.80 mm compared to some of the modes with low frequencies. It was again observed that the deformation of the connecting rod of aluminium 7075 T6 alloy material is not proportional to the magnitudes of the natural frequencies.

3.2. Comparison of Deformations and Natural Frequencies

The deformations and natural frequencies of the connecting rods made with the four different materials were compared using Figure 8 as shown.

Figure 8 presents the comparison of deformations of the connecting rods made with the four different materials were compared, it was observed that the connecting rod made with aluminium 7075 alloy yielded the highest deformations across all mode levels. It was also observed that mode number 5 yielded the least deformation of 85.416 mm whiles mode number 9 yielded the highest deformation of 172.44 mm within the ten (10) mode levels of the aluminium 7075 alloy material. Figure 8 also shows that titanium alloy connecting rod also significantly deformed but not as compared to aluminium 7075 alloy connecting rod. It was also revealed that mode number 5 has the least deformation of 66.588 mm whiles mode number 9 yielded the highest deformation of 134. 74 mm within the ten (10) mode levels of titanium alloy material. The results also show almost the same levels of deformation for structural steel and gray cast iron connecting rods but with careful observation, structural steel appeared to have the least deformations across all mode levels. The deformations of the connecting rods of the four materials appeared to follow the same trend as in all cases, mode numbers 5 having the lowest deformations while mode numbers 9 having the highest deformations. The deformations were observed to be trending downward at mode number 10. The comparison revealed that structural steel and gray cast iron materials have superior properties to resist deformation than aluminium 7075 and titanium alloy materials. If a connecting rod were to be selected based on deformation, the ranking would have been first structural steel, gray cast iron, titanium alloy and aluminium 7075 alloy respectively.

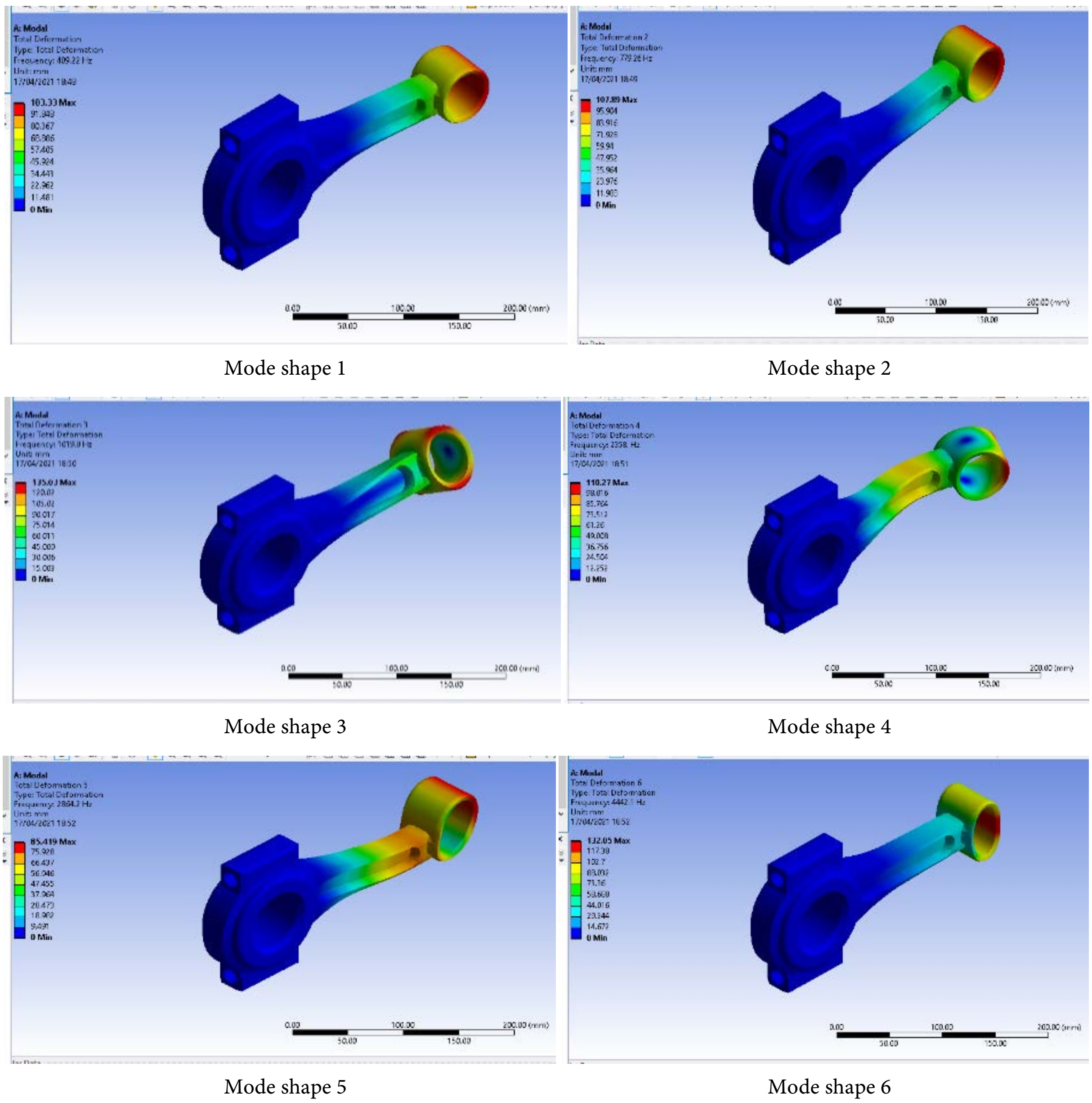

Figure 7. Mode shapes from 1 to 6 for Al 7075 alloy.

Table 8. Deformations and natural frequencies of connecting rod of aluminium Al7075.

Mode number	Aluminium 7075 T6 Material	
	Deformation (mm)	Natural frequency (Hz)
1	103.33	409.22
2	107.89	779.26
3	135.03	1019.80
4	110.27	2358.00
5	85.419	2864.20
6	132.05	4442.10
7	137.97	5364.30
8	99.36	6302.10
9	172.44	6820.50
10	102.80	7957.00

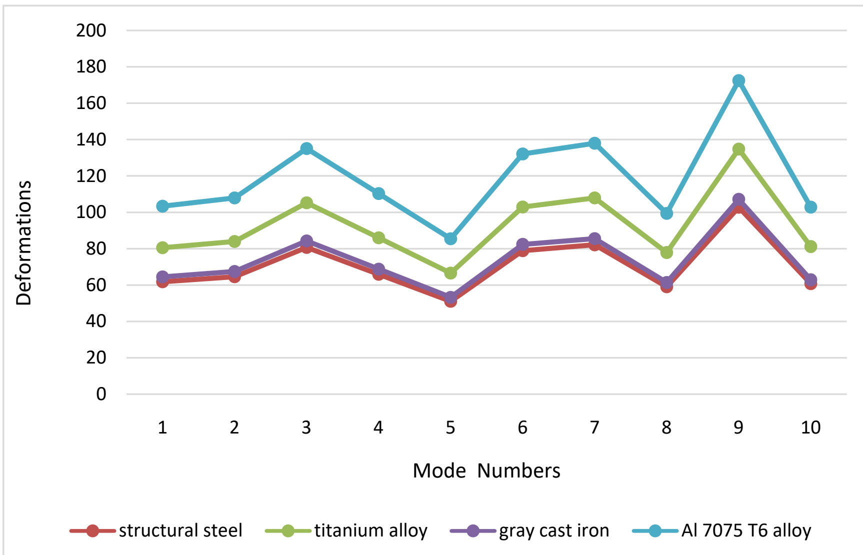

Figure 8. Comparison of deformations of Con. rod for all the four materials.

Figure 9 compares the natural frequencies of the free vibrations of the connecting rods of the four different connecting rod materials at no-load conditions. The trend as shown in the graph indicates that the natural frequencies increase along with an increasing mode numbers. **Figure 9** shows that aluminium 7075 alloy connecting rod has the highest natural frequencies at all levels of mode numbers ranging from mode 1 to 10. When the highest vibrational frequencies corresponding to mode 10, of all the connecting rod materials were compared the frequencies obtained were: aluminium 7075 alloy connecting rod produced 7957 Hz, structural steel material connecting rod produced 7920.1 Hz, titanium alloy material connecting rod produced 7196.4 Hz and gray cast iron material connecting rod produced 6123 Hz respectively. The **Figures 10-13** shows that gray cast iron material connecting rod produced the lowest vibrational natural frequencies at all levels of mode numbers. Aluminium 7075 alloy connecting rod and structural steel material connecting rods appear to have superior properties in terms of vibrations than gray cast iron material connecting rod (Tables 9-13.)

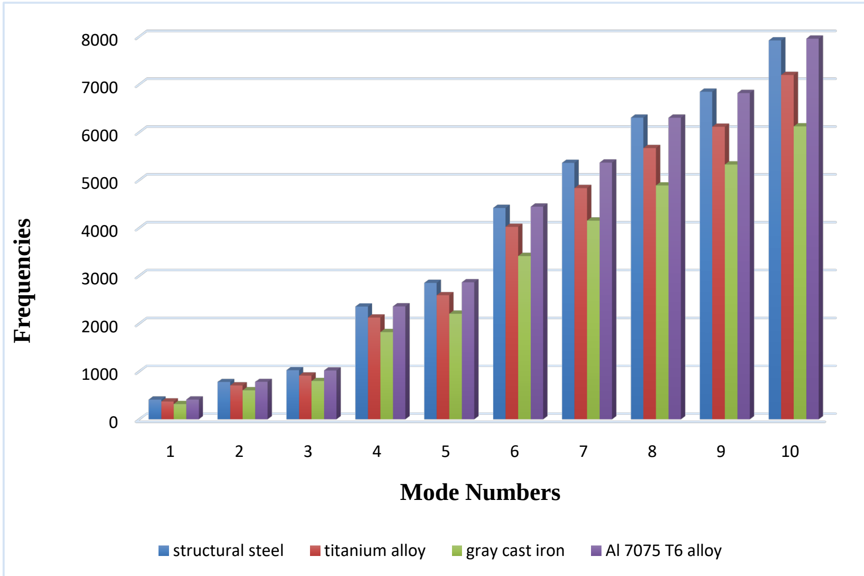

Figure 9. Comparison of natural frequencies of connecting rod materials.

3.3. Thermal Analyses of the Connecting Rod

Structural steel

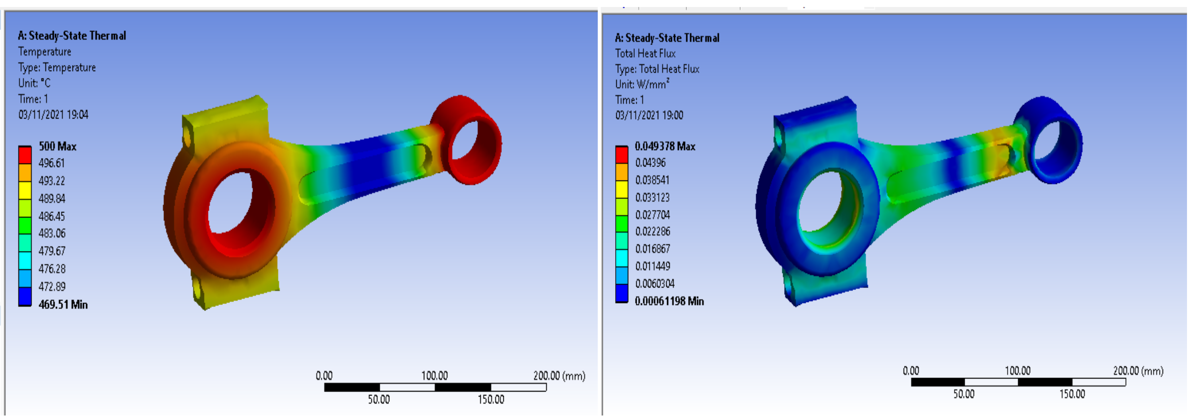

Temperature | Total heat flux

Figure 10. Contour plot for temperature, total heat flux for structural steel.

Table 9. Thermal analysis results for structural steel Con. rod.

	Temperature ˚C	Total Heat Flux W/mm²
Maximum	500	0.049378
Minimum	469.51	0.00061198

Titanium alloy

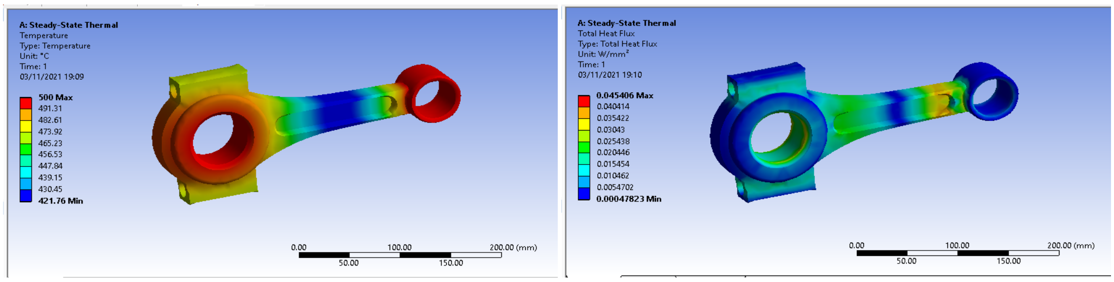

Temperature Total heat flux

Figure 11. Contour plot for temperature, total heat flux for titanium alloy.

Table 10. Thermal analysis results for titanium alloy Con. rod.

	Temperature ˚C	Total Heat Flux W/mm^2
Maximum	500	0.045406
Minimum	421.76	0.00047823

Gray cast iron

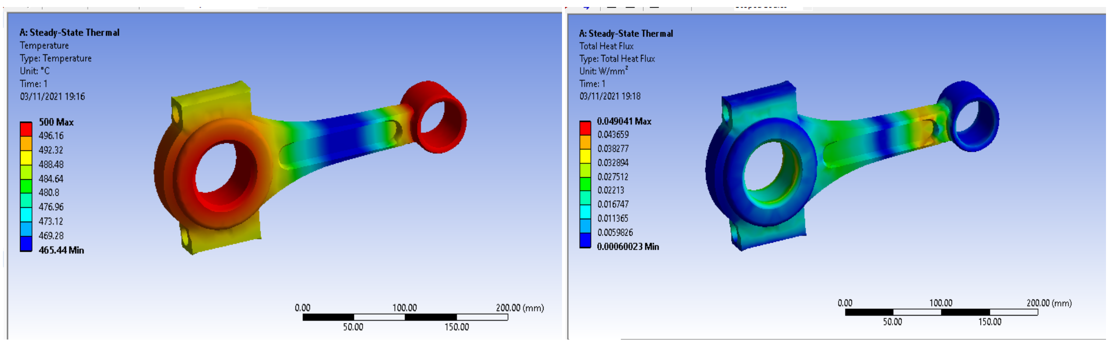

Temperature Total heat flux

Figure 12. Contour plot for temperature, total heat flux and directional heat for grey cast iron.

Table 11. Thermal analysis results for gray cast iron Con. rod.

	Temperature ˚C	Total Heat Flux W/mm^2
Maximum	500	0.049041
Minimum	469.28	0.00060023

Aluminium Alloy 7075

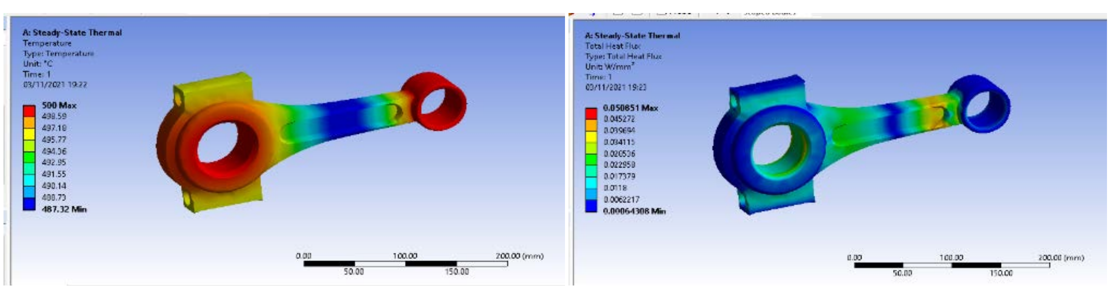

Temperature Total heat flux

Figure 13. Contour plot for temperature, total heat flux and directional heat for Al 7075.

Table 12. Thermal analysis results for aluminium alloy 7075 Con. rod.

	Temperature ˚C	Total Heat Flux W/mm^2
Maximum	500	0.050851
Minimum	487.32	0.00064308

Table 13. Summary of thermal analysis results for all materials.

Materials		Temperature ˚C	Total Heat Flux W/mm^2
Structural steel	Maximum	500	0.049378
	Minimum	469.51	0.000612
Titanium alloy	Maximum	500	0.045406
	Minimum	421.76	0.000478
Gray Cast Iron	Maximum	500	0.049041
	Minimum	469.28	0.000600
Aluminium Alloy 7075	Maximum	500	0.050851
	Minimum	487.32	0.000643

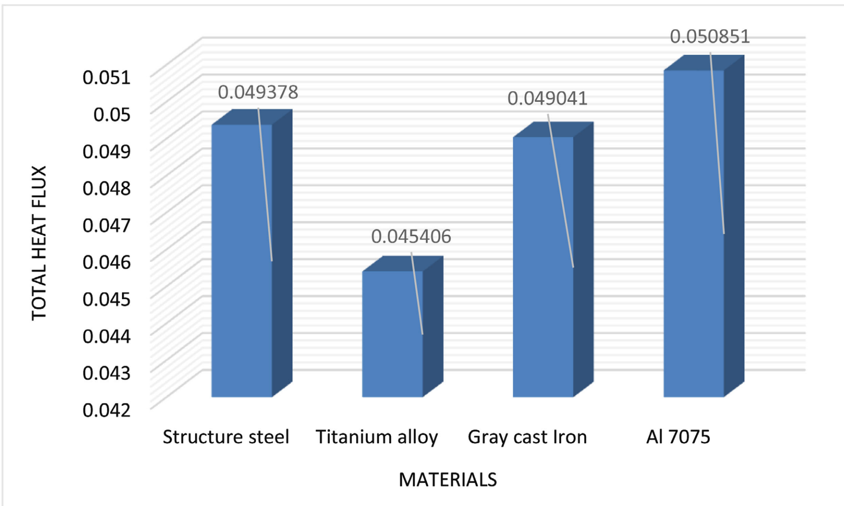

Figure 14. Comparison of Total Heat Flux for all Materials.

From Figure 14, it can be seen that aluminium 7075 alloy has the highest total heat flux of 0.050851 W/mm^2. It implies that aluminium 7075 alloy connecting rod tends to dissipate more heat than the other materials. There is a faster rate of transfer of heat from the connecting rod to its surroundings making it one of the best materials for connecting rod design and manufacture. Structural steel and gray cast iron materials connecting rod have a total heat flux of 0.049378 W/mm^2 and 0.049041 W/mm^2 respectively. Figure 14 also shows that the two materials which are structural steel and gray cast iron materials have similar heat properties and are both good for connecting rod manufacture. The results show that the material with the least total heat flux is titanium alloy which has a total heat flux magnitude of 0.045406 W/mm^2.

4. Conclusion

This study considered modal and thermal analyses to investigate the suitability of al 7075 materials for connecting rod design. The parameters that were considered under the modal analysis were: total deformation and natural frequency, while the thermal analysis looked at the temperature distribution, and total heat flux of the four connecting rods made with titanium alloy, gray cast iron, structural steel and aluminium 7075 alloy respectively. The main objective of this work was to determine the possibility of using aluminium alloy 7075 material to design and manufacture a connecting rod for weight optimisation without losing the strength of the connecting rod. The connecting rod was modelled using Autodesk inventor 2017 software using the calculated dimensions. The dimensioning of the connecting rod was obtained through systematic and rigorous calculations based on theoretically empirical formulas for connecting rod design. The analysis of the connecting rod was done using Ansys software. The results compared for the materials showed that aluminium 7075 alloy material yielded the highest deformation of 172.44 mm while structural steel and gray cast iron yielded the least deformation making them have superior qualities to resist deformation more than aluminium 7075 and titanium alloys. However, aluminium 7075 alloy proved to have superior qualities in thermal parameters than the other materials making aluminium 7075 alloy material one of the best materials for connecting rod design and manufacture. The connecting rod should have been tested in a functional engine to determine its feasibility. Future work into connecting rod design using the same material should consider testing the connecting road in a functional internal combustion engine.

Conflicts of Interest

The authors declare no conflicts of interest regarding the publication of this paper.

References

[1] Hillier, V.A.W. and Coombes, P. (2004) Hillier's Fundamentals of Motor Vehicle Technology. Nelson Thornes, Cheltenham.

[2] Witek, L. and Zelek, P. (2019) Stress and Failure Analysis of the Connecting Rod of Diesel Engine. *Engineering Failure Analysis*, **97**, 374-382. https://doi.org/10.1016/j.engfailanal.2019.01.004

[3] Mohankumar, D., Rakesh, M.L. and Bist, B. (2017) Design and Analysis of a Connecting Rod. *International Journal of Pure and Applied Mathematics*, **116**, 105-109.

[4] Dale, J.R. (2005) Connecting Rod Evaluation. Metal Powder Industries Federation, New York.

[5] Khurmi, R. and Gupta, J. (2005) A Textbook of Machine Design Text of Machine Design. Eurasia Publishing House (Pvt.) Ltd., New Delhi.

[6] Sathish, T., Kumar, S.D. and Karthick, S. (2020) Modelling and Analysis of Different Connecting Rod Material through Finite Element Route. *Materials Today: Proceedings*, **21**, 971-975. https://doi.org/10.1016/j.matpr.2019.09.139

[7] Nitturkar, H.D., Kalshetti, S.M. and Nadaf, A.R. (2020) Design and Analysis Connecting Rod Using Different Materials. *International Research Journal of Engineering and Technology*, **7**, 1011-1017.

[8] Shenoy, P.S. and Fatemi, A. (2005) Connecting Rod Optimization for Weight and Cost Reduction. *SAE Transactions*, **1**, 523-530. https://doi.org/10.4271/2005-01-0987

[9] Grover, K. and Budania, B. (2012) Optimization of Connecting Rod Parameters Using CAE Tools.

[10] Dupare, Y.B., Tirpude, R.B. and Bharadbhunje, A.Y. (2014) Fatigue Analysis in Connecting Rod Using ANSYS. *Scientific Journal*, **4**, 215-220.

[11] Abhinav Gautam, K. and Ajit, P. (2013) Static Stress Analysis of Connecting Rod Using Finite Element Approach. *IOSR Journal of Mechanical and Civil Engineering* (*IOSR-JMCE*), **10**, 47-51. https://doi.org/10.9790/1684-1014751

[12] Doshi, N. and Ingole, N. (2013) Analysis of Connecting Rod Using Analytical and Finite Element Method. *International Journal of Modern Engineering Research*, **3**, 65-68.

[13] Balli, S.R., Shetty, P. and Sajjan, S. (2020) Design, Analysis and Comparison of Various Materials for Connecting Rod. *EPRA International Journal of Research and Development* (*IJRD*), **5**, 53-61.

[14] Fukuda, S. and Eto, H. (2002) Development of Fracture Splitting Connecting Rod. *JSAE Review*, **23**, 101-104. https://doi.org/10.1016/S0389-4304(01)00154-0

[15] Buddi, T., Rana, R., Sikarwar, D.S., Rajesh, K.D. and Dhakad, S. (2020) Design and Comparative Performance Analysis of Two Wheeler Connecting Rod with Silicon Nitride and Aluminum7068 by Finite Element Analysis.

[16] Muhammad, A., Ali, M. and Shanono, I. (2020) Finite Element Analysis of a Connecting Rod in ANSYS: An Overview. *IOP Conference Series*: *Materials Science and Engineering*, **2020**, Article ID: 022119. https://doi.org/10.1088/1757-899X/736/2/022119

[17] Ajit, K. and Ravindra, M. (2019) Thermal Transient Analysis on Connecting Rod Using Finite Element Analysis. *International Journal of Recent Technology Science and Management*, **4**, 2455-9679.

[18] Sunny, K., Maneesh, S. and Rajneesh, K.G. (2019) Thermal Transient Analysis on Connecting Rod Using Finite Element Analysis. *International Journal of Recent Technology Science and Management*, **4**, 622-633.

[19] Vali, D.S., Premkumar, T.M., Sai, A.A., Sudarshan, P., Roopak, P., Hariram, V., *et al.* (2021) Finite Element Analysis of the Thermal Behaviour of Different Types of Connecting Rod for Various Materials. *International Journal of Vehicle Structures & Systems* (*IJVSS*), **13**, 510-513. https://doi.org/10.4273/ijvss.13.4.21